

# Thermodynamics of Random Ferromagnetic Antiferromagnetic Spin-1/2 Chains

Beat Frischmuth<sup>1</sup>, Manfred Sigrist<sup>2</sup>, Beat Ammon<sup>1</sup> and Matthias Troyer<sup>3</sup>

<sup>1</sup> *Institute of Theoretical Physics, ETH Hoenggerberg, CH-8093 Zuerich, Switzerland*

<sup>2</sup> *Yukawa Institute for Theoretical Physics, Kyoto University, Kyoto 606-01, Japan*

<sup>3</sup> *Institute for Solid State Physics, University of Tokyo, Roppongi 7-22-1, Tokyo 106, Japan*

(May 17, 2018)

Using the quantum Monte Carlo Loop algorithm, we calculate the temperature dependence of the uniform susceptibility, the specific heat, the correlation length, the generalized staggered susceptibility and magnetization of a spin-1/2 chain with random antiferromagnetic and ferromagnetic couplings, down to very low temperatures. Our data show a consistent scaling behavior in all the quantities and support strongly the conjecture drawn from the approximate real-space renormalization group treatment. A statistical analysis scheme is developed which will be useful for the search of scaling behavior in numerical and experimental data of random spin chains.

## I. INTRODUCTION

Over many decades one-dimensional (1D) quantum spin systems have attracted much interest. Despite of their simplicity they show a wealth of physical properties which provide many keys to the understanding of phenomena appearing also in other strongly correlated systems. Since the discovery of various quasi-1D materials the study of 1D spin systems, mainly based on the Heisenberg model and its variations, is also of experimental relevance. Examples of such materials include the so-called NINO ( $\text{Ni}(\text{C}_3\text{H}_{10}\text{N}_2)_2\text{NO}_2(\text{Cl})_4$ ), NENP ( $\text{Ni}(\text{C}_2\text{H}_8\text{N}_2)_2\text{NO}_2(\text{Cl})_4$ ),<sup>1,2</sup> and  $\text{Sr}_3\text{CuPtO}_6$ .<sup>3</sup> In particular, the latter system belongs to a class of compounds which is compositionally very flexible. It is possible to produce compounds of the form  $\text{Sr}_3\text{MNO}_6$  in various combinations with  $\text{M}=\text{Cu, Mg, Zn, Yb, Na, Ca, Co, and N}=\text{Pt, Ir, Rh, Bi}$ . Other examples are the spin ladder systems, such as  $\text{Sr}_{n-1}\text{Cu}_{n+1}\text{O}_{2n}$  ( $n+1$ , the number of ladder legs) or  $\text{CaV}_2\text{O}_5$ .<sup>4</sup>

Disorder effects play a particularly important role in quasi-1D systems, because even small deviations from regularity often destabilize the pure phases.<sup>5</sup> Real experimental systems naturally contain impurities and other types of disorder. Therefore it is very important to understand the influence of disorder on the properties of such systems in order to interpret experimental results.

This is one reason why in recent years random spin systems have been investigated intensively. But also from the theoretical point of view, random spin systems are interesting since they provide a simple model to study the interplay between quantum effects and disorder. There are various realizations of quasi-one-dimensional random spin systems in nature. One class is represented by compounds like  $\text{Sr}_3\text{CuPt}_{1-x}\text{Ir}_x\text{O}_6$ .<sup>6</sup> While the pure compounds  $\text{Sr}_3\text{CuPtO}_6$  ( $x=0$ ) and  $\text{Sr}_3\text{CuIrO}_6$  ( $x=1$ ) are antiferromagnetic (AFM) and ferromagnetic (FM), respectively, the alloy  $\text{Sr}_3\text{CuPt}_{1-x}\text{Ir}_x\text{O}_6$  contains both AFM and FM couplings whose fraction is simply related to the concentration  $x$  of Ir. A corresponding minimal model of this type is the spin-1/2 Heisenberg

chain, where the nearest neighbor exchange coupling is  $+J$  or  $-J$  with certain probabilities.<sup>7</sup> Another related example is realized in the low-temperature regime of randomly depleted AFM spin-1/2 Heisenberg ladders. Two-leg Heisenberg ladders have a resonating valence bond ground state which has short-range singlet correlation and a spin excitation gap.<sup>4</sup> If spins are depleted at random the low-energy properties are changed drastically. Each site which lost a spin is accompanied by an effective spin 1/2, and the residual interaction among these spins is randomly FM or AFM with a wide distribution of coupling strengths.<sup>8,9</sup> Recently, it was also shown that random AFM spin-1 chains including next-nearest neighbor couplings can generate effective ferromagnetic couplings in the low-energy regime so that they should behave similarly at low-temperature.<sup>10</sup>

In this work we focus on random FM-AFM spin chains with the full spin rotation symmetry. One of the most insightful techniques to study such systems is the real space renormalization group (RSRG) method.<sup>11-17</sup> This method was introduced to study random AFM spin-1/2 chains,<sup>11-15</sup> and was recently adapted to the study of the class of systems introduced above.<sup>16,17</sup> The basic idea of the RSRG method is the iterative decimation of degrees of freedom by successively integrating out the strongest bonds in the spin chain. In this way the distribution of coupling strengths and spin sizes is renormalized. For many cases an universal fixed point distribution is reached in the low-energy limit. The random AFM spin-1/2 chain belongs to a universality class different from that of the random FM-AFM spin chain. The former is characterized by a *random singlet phase* where each spin tends to form a singlet with one other spin even over very large distances. For the FM-AFM spin chain, however, spins correlate to form effective spins whose average size grows with lowering of the energy scale.<sup>16-18</sup> A result of the RSRG method is that the average number of original spins included in a single effective spin for a given (energy or) temperature  $T$  scales as  $\bar{l} \propto T^{-2\alpha}$ , and the average spin size  $\bar{S} \propto T^{-\alpha}$  for  $T \rightarrow 0$ .<sup>16,17</sup>

We start our analysis with a brief review of the RSRG

scheme and its results<sup>16,17</sup> for the random FM-AFM spin chain which shows a universal scaling behavior at low-temperatures (section 4.2). The RSRG treatment, however, relies on certain approximations which have not so far been independently tested. We use, therefore, a different approach to examine the random FM-AFM spin-1/2 chain and the validity of the scaling assumption underlying the RSRG scheme.<sup>19</sup> For the analysis of the numerical data obtained by the continuous time version of the quantum Monte Carlo (QMC) loop algorithm<sup>20,21</sup> we introduce a statistical description of the low-temperature properties (section 4.3). Various quantities such as the uniform susceptibility, specific heat, generalized staggered susceptibility, correlation and generalized staggered magnetization are discussed in section 4.4. We find excellent agreement between our analysis and the RSRG treatment by Westerberg *et al.*<sup>16,17</sup> Beyond the consistent evaluation of the scaling exponent  $\alpha$ , our simulation gives quantities mentioned above over a wide range of temperatures and our discussion provides a technique to analyze (numerical or experimental) data for the low-temperature scaling regime.

## II. REAL SPACE RENORMALIZATION GROUP TREATMENT

The real space renormalization group scheme used by Westerberg *et al.*<sup>16,17</sup> can be applied to the large class of random spin systems with a Hamiltonian of the form

$$H = \sum_i J_i \vec{S}_i \cdot \vec{S}_{i+1}, \quad (1)$$

where the strength and sign of  $J_i$  as well as the size of the spins  $S_i$  are randomly distributed according to the distributions  $P(J)$  and  $\tilde{P}(S)$ , respectively. The basic idea of the RSRG method is the iterative decimation of degrees of freedom by integrating out successively the strongest bonds in the spin chain. The RG step will now be described in more detail.

For this purpose a bond in the chain is defined as two neighboring spins and the coupling  $J$  connecting them. If a bond is isolated from the rest of the chain, it would form a local ground state of maximum ( $J < 0$ ) or minimum ( $J > 0$ ) spin with an energy gap  $\Delta$  to the first excited multiplet. For a FM bond  $\Delta = -J(S_L + S_R)$ , while for an AFM bond  $\Delta = J(|S_L - S_R| + 1)$ , where  $S_L$  and  $S_R$  are the left and right spins of the bond, respectively. Now we focus on the strongest bond in the chain, defined as the bond with the largest gap  $\Delta = \Delta_0$ . If the distribution of gaps is broad (this is the case if the coupling strength and/or the spin-size distribution is broad), the gaps of the two neighboring bonds,  $\Delta_1$  and  $\Delta_2$ , are typically much smaller than  $\Delta_0$  so that the two spins  $S_L$  and  $S_R$ , to a good approximation, lock into their local ground state. Consequently, the bond  $\Delta_0, S_L, S_R$  is

replaced by a single effective spin  $S' = |S_L \pm S_R|$  representing the local ground state of minimum (AFM) or maximum (FM) spin. The weaker neighboring bonds are then taken into account perturbatively in  $\Delta_{1,2}/\Delta_0$ , leading to an effective interaction between the spins  $S_1, S'$ , and  $S_2$  (see Fig. 1). The spin rotation symmetry is preserved in this procedure, and to first order in  $\Delta_{1,2}/\Delta_0$  no next-nearest neighbor interactions are generated. At this point, however, it is important to note that the crucial assumption of  $\Delta_1, \Delta_2 \ll \Delta_0$  is probable, but uncontrolled and independent tests are necessary to examine whether this assumption and, hence, the RSRG results are correct (section 4.3 and 4.4).

Integrating out the strongest bond successively in the manner described above preserves the the form of the Hamiltonian Eq. (1) but changes the coupling strength distribution, the spin distribution and in particular reduces the energy scale  $\Delta_0$ . We expect that after many iteratively performed decimation steps the distributions flow to a fixed-point distributions with universal scaling behavior. According to Westerberg *et al.*,<sup>16,17</sup> these fixed point distributions are universal for a large class of initial  $P(J)$  and  $\tilde{P}(S)$ , namely if the initial gap distribution  $\hat{P}(\Delta)$  is regular or less singular than  $\hat{P}(\Delta) \sim \Delta^{-0.7}$ .

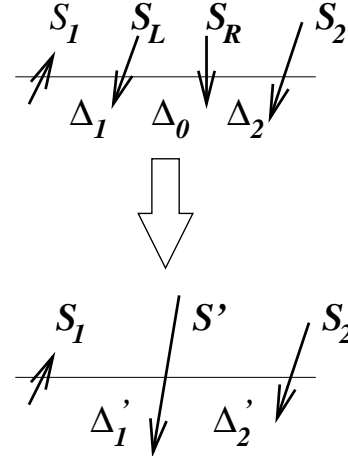


FIG. 1. Schematic picture of one step in the RSRG treatment of Westerberg *et al.*<sup>16,17</sup>

The RSRG results<sup>16,17</sup> show that for this whole class of distributions the average number  $\bar{l}$  of original spins included in one effective large spin diverges with  $\Delta_0^{-2\alpha}$  as  $\Delta_0 \rightarrow 0$  with an universal exponent  $\alpha = 0.22 \pm 0.01$ . The total spin of an effective large spin is the sum of the participating original spins, where each spin enters the sum with the (opposite) sign as its neighbor if the coupling is ferromagnetic (antiferromagnetic). By a random walk argument one finds for the average total quantum spin number  $\bar{S}$

$$\bar{S} \propto \sqrt{\bar{l}} \propto \Delta_0^{-\alpha}. \quad (2)$$

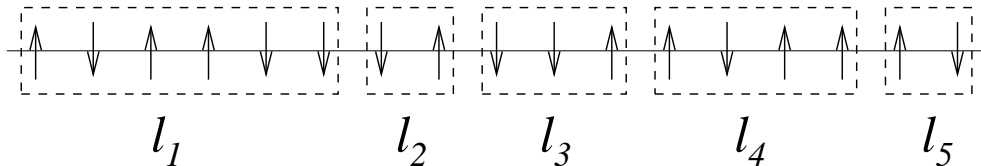


FIG. 2. Possible cluster forming at given temperature  $T$ . The cluster lengths  $l_1, l_2, \dots$  are exponentially distributed with an average value  $\bar{l} = \lambda^2(T/J_0)^{-2\alpha}$

At finite temperature  $T$  the RG flows will stop at  $\Delta_0 \sim k_B T$ . All bonds with a gap larger than  $\Delta_0$  are essentially frozen to form effective large spins which are, in turn, more or less independent from each other. These free effective spins lead to a Curie like behavior of the magnetic uniform susceptibility  $\chi$  per unit length for  $T \rightarrow 0$ , since the scaling behavior of  $\bar{S}^2$  and  $\bar{l}$  is identical,

$$\frac{\chi}{L} = \frac{\mu^2}{3k_B T} \frac{\bar{S}^2}{\bar{l}} \propto \frac{1}{T} \frac{\Delta_0^{-2\alpha}}{\Delta_0^{-2\alpha}} = \frac{1}{T}. \quad (3)$$

For the entropy  $\sigma$  (per original spin) we can argue that only the free effective spins contribute such that

$$\sigma = \frac{\bar{l}}{k_B} \ln(2\bar{S} + 1) \propto T^{2\alpha} \ln T \quad (4)$$

in leading order, which is identical to that of the specific heat  $C$  per spin.

In summary we have the following physical picture of the RSRG scheme. At a given finite temperature  $T$ , the original spins are grouped in completely correlated clusters forming an effective spin. These clusters are independent and have an average length  $\bar{l} \propto T^{-2\alpha}$ . This will be the basis of our statistical approach for the discussion of the thermodynamic properties.

### III. METHODS

#### A. Quantum Monte Carlo calculations

For the numerical simulation we use as model a FM-AFM spin-1/2 chain

$$H = \sum_i J_i \vec{S}_i \vec{S}_{i+1}, \quad (5)$$

where  $\vec{S}_i$  is the  $i^{\text{th}}$  spin of the chain and  $J_i$ , the coupling strength of the  $i^{\text{th}}$  bond, takes random values of both positive and negative sign. We assume the bond distribution

$$P(J) = \begin{cases} \frac{1}{2J_0} & -J_0 < J < J_0 \\ 0 & \text{otherwise,} \end{cases} \quad (6)$$

where  $J_0$  is the maximal coupling setting the energy scale.

According to Westerberg *et al.*,<sup>17</sup> the low energy behavior of the random FM-AFM chain is independent of the initial distribution as long as  $J^{y_c} P(J)$  is regular for  $J \rightarrow 0$  with  $y_c \approx 0.7$ . Our choice particular distribution [Eq. (6)] is guided by the feasibility for the numerical analysis of the scaling regime. This does not restrict the validity of the conclusions since the scaling behavior should be universal for all distributions in above class. Distribution functions closer to those of the real systems mentioned in the introduction, on the other hand, while interesting to study in connection with experiments on real material<sup>22</sup>, are not suitable for an accurate analysis of the scaling regime, since the scaling regime occurs at much lower temperature relative to the characteristic coupling strength  $J_0$ .

Using the QMC loop method<sup>20,21</sup>, we simulate 100 samples of spin chains of 400 sites in a temperature range down to temperatures as low as  $T = J_0/1000$ . In the QMC loop algorithm the calculations are performed directly with a Trotter time interval  $\Delta\tau = 0$ , so no extrapolation in the Trotter time interval is necessary (see section 2.7). To obtain good statistics, we consider 100 different realizations of random coupling spin chains, following the distribution in Eq. (6). The temperature dependences of the physical properties are calculated for each chain separately, and then averaged over the 100 samples.

#### B. Statistical cluster analysis

The fact that the correlation of spins occurs within definite clusters permits the use of a special statistical approach for the discussion of the thermodynamic properties. Original spin-1/2s belonging to the same cluster are completely correlated, while correlations between original spins belonging to different cluster can assumed to be zero (c.f. Fig. 2). Therefore, the contributions of these frozen clusters to a physical observable  $\mathcal{A}$  can be considered independently and be estimated simply as the zero-temperature (ground state) value within each cluster (depending only on their length  $l$ ).

Performing a statistical analysis of the cluster length  $l$  allows to go beyond the leading order in the temperature dependence of  $\chi$  and  $\sigma$ , as predicted by the RSRG [Eq. (3) and Eq. (4)], as well as to calculate also the  $T$ -

dependence of other physical quantities. Namely, the low temperature dependence of physical observable  $\mathcal{A}$  per site in a random AFM-FM spin-1/2 chain of length  $L \gg 1$  can be expressed as

$$A(T) = \frac{1}{L} \sum_{l=1}^{\infty} n_T(l) l \mathcal{A}_l, \quad (7)$$

where  $n_T(l)$  is the number of clusters of length  $l$  and  $\mathcal{A}_l$  is the zero-temperature (ground state) value of  $\mathcal{A}$  per site for such a cluster. As  $L$  goes to infinity, we define the probability distribution  $p_T(l)$  of the cluster length  $l$  to appear at given temperature  $T$ , as  $p_T(l) \equiv n_T(l) / \sum_l n_T(l)$ . The total number of clusters  $\sum_l n_T(l)$  is equal to  $L/\bar{l}$ , where  $\bar{l}$  is the average cluster length. Hence

$$A(T) = \frac{1}{\bar{l}} \sum_{l=1}^{\infty} p_T(l) l \mathcal{A}_l. \quad (8)$$

As mentioned above, the RSRG approach predicts a power-law scaling behavior for the temperature dependence of  $\bar{l}$ ,

$$\bar{l} = \lambda^2 \left( \frac{T}{J_0} \right)^{-2\alpha}, \quad (9)$$

where  $\lambda$  is a dimensionless proportionality factor.

Let us now consider the distribution of cluster lengths  $l$  for a given temperature. It is natural to assume that the bonds freeze uncorrelated to each other, i.e. each bond is frozen with a certain probability independent of the location within the chain. Thus, the distribution  $p_T(l)$  of the cluster length  $l$  has an exponential form. Its average value  $\bar{l}$  is given by Eq. (9) and, hence, we will write  $p_{\bar{l}}(l) \equiv p_T(l)$  in the following. The distribution  $p_{\bar{l}}(l)$  has to be normalized for a sum over  $l$  from 1 to  $\infty$  and reads in its discrete form

$$p_{\bar{l}}(l) = (e^{\kappa} - 1) e^{-\kappa l}, \quad \text{with } \kappa = \log\left(1 + \frac{1}{\bar{l} - 1}\right). \quad (10)$$

The distribution  $\rho_l(S)$  of the spin size of a cluster of fixed length  $l$  also plays an important role, since the contribution  $\mathcal{A}_l$  to many physical observables can be determined using  $\rho_l(S)$ . The effective spin of a cluster of length  $l$  is equal to the ground state spin quantum number  $S$ . For spin-1/2 degrees of freedom coupled randomly by FM or AFM bonds the probability distribution for these quantum numbers is given by (an explanation is presented below)

$$\rho_l(S) = \frac{l!}{(l/2 + S)!(l/2 - S)!} \frac{1}{2^l} (2 - \delta_{S,0}), \quad (11)$$

where for even  $l$ ,  $S$  is integer with  $0 \leq S \leq l/2$  and for odd  $l$ ,  $S$  is half-integer with  $\frac{1}{2} \leq S \leq l/2$ . Because the system contains no frustrating couplings, the spin quantum number  $S$  is identical to the total spin of the corresponding completely correlated cluster of classical

spins.<sup>23</sup> The total spin of a classical cluster of length  $l$ , however, can easily be calculated. It is the sum of all original spins 1/2, where each spin enters the sum with the same (opposite) sign as its neighbor if the bond is ferromagnetic (antiferromagnetic). The summation therefore can be visualized by a random walk on a 1D lattice. A ferromagnetic (antiferromagnetic) bond corresponds to a step of one lattice constant to the left (right). The random walk contains of  $l$  steps and the distance between the end point of the random walk and the origin in the 1D lattice is equal to  $2S$  and the distribution  $\rho_l(S)$  [Eq. (11)] gives the probability for such a random walk.

The two distributions  $p_{\bar{l}}(l)$  [Eq. (10)] and  $\rho_l(S)$  [Eq. (11)] together with the scaling behavior of  $\bar{l}$  [Eq. (9)] are sufficient to calculate the low-temperature thermodynamics of various physical quantities. This will be done in the next section for the uniform susceptibility, specific heat, entropy and correlation length.

## IV. RESULTS

### A. Intermediate temperature regime

Before turning to the main point of this chapter, the study of the universal low- $T$  scaling regime, we will concentrate on the intermediate temperature range of the random FM-AFM spin-1/2 chains. The behavior in this range and the way entering the universal low- $T$  are both strongly dependent on the initial coupling distribution function  $P(J)$ . To study these points, in this subsection, we choose different initial coupling distribution functions  $P(J)$  having a width  $\int_{-\infty}^{\infty} dJ |J| P(J) = J_0/2$  and being normalized to one ( $\int_{-\infty}^{\infty} dJ P(J) = 1$ ).

First we investigate the uniform Curie constant  $T\chi(T)$ , as a measure for the still uncorrelated spins at a given temperature, considering random FM-AFM spin chains of four sites with open boundary conditions. For these systems the bond average can be performed exactly and the calculations take only little time. Thus a more extended study of the dependence of the behavior on the initial coupling distribution  $P(J)$  in the intermediate temperature range is possible. It is clear that finite size effects allow only a qualitative study of this problem, but the main characteristic features can already be seen in the 4-site chain.

The principal process leading to the dependence of the uniform Curie constant on the initial coupling distribution function is the following: For a given temperature the bonds which had a coupling  $J \gtrsim T$  are frozen either into a singlet (AFM bond) or a triplet (FM bond) configuration. Thus, an uncorrelated bond contributes 1/2 to  $T\chi$ , a triplet bond 2/3 and a singlet zero (we set the Bohr magneton to unity). Thus, the average contribution per bond is reduced if the FM and AFM couplings occur with the same probability, as considered here. The decrease of  $T\chi$  corresponds to the rate of freezing of bonds as

the temperature is lowered, i.e. the constant distribution function leads to a linear temperature dependence, as observed for the box distribution (see Fig. 3 and Fig. 5). For the roof distribution (shown in the inset of Fig. 3), compared with the box distribution, the deviation from the free spin-1/2 limit of  $1/4$  starts at higher temperature, since the largest possible coupling in the chain is larger for the roof than for the box distribution. In the intermediate temperature range ( $0.1J_0 \lesssim T \lesssim 0.5J_0$ ) the decrease of the Curie constant for the roof distribution with decreasing  $T$  is first smaller than for the box distribution, but then increases and entering the low temperature regime it is again larger than for the box distribution, as expected from the shape of both initial coupling distributions (see Fig. 3). Here, the low- $T$  regime means the temperature range, where not only single bonds are frozen, but all four spins start to be correlated and renormalization effects of the distribution function becomes visible.

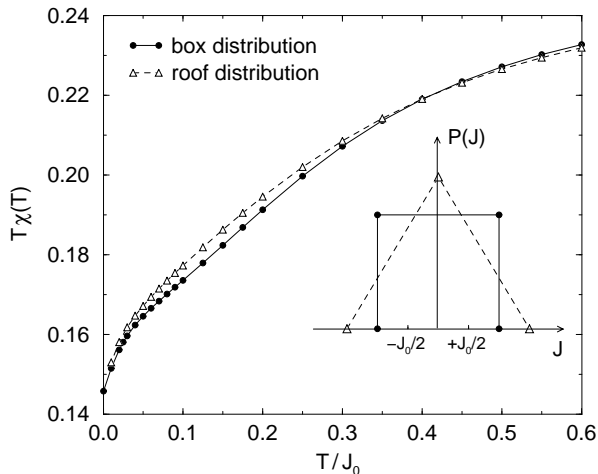


FIG. 3. Temperature dependence of the uniform Curie constant  $T\chi(T)$  for 4-site random spin chains with initial coupling distribution function  $P(J)$  shown in the inset (box and roof form).

In a second step we analyze the effect of an initial coupling distribution  $P(J)$  which is no longer broad but rather peaked at some values  $J \neq 0$ . In Fig. 4 the temperature dependence of the Curie constants for 4-site chains with initial coupling distributions

$$P(J) = \begin{cases} \frac{1}{4\delta J_0} & \text{if } (\frac{1}{2} - \delta)J_0 < |J| < (\frac{1}{2} + \delta)J_0 \\ 0 & \text{otherwise,} \end{cases} \quad (12)$$

for different  $\delta = 0, 0.05, 0.25, 0.4, 0.5$  are shown. The case  $\delta = 0$  corresponds to a random chain with couplings  $\pm J_0/2$ , while the case with  $\delta = 0.5$  represents the box distribution Eq. (6). The latter was already discussed above. The other broad distribution  $\delta = 0.4$  leads to a very similar behavior in  $T\chi$  to the box distribution and

the small differences can be explained by the same argument as before. The random spin chains with peaked initial  $P(J)$  ( $\delta = 0.05$  and  $0$ ), however, behave completely different in the intermediate temperature range. As all couplings are approximately of the same strength, the picture of successively freezing of the strongest bond with lowering temperature no longer applies. According to Furusaki *et al.*<sup>7</sup> in such random chains, in the intermediate temperature regime all sequences of only AFM and of only FM bonds lock together, forming new effective spins of random spin size and which are coupled very weakly according to a new and broad coupling distribution. This forming of weakly interacting effective spins is indicated by the plateau in the uniform Curie constant (see Fig. 4). As the temperature is lowered further, the effective spins start to correlate and the Curie constant decreases again.

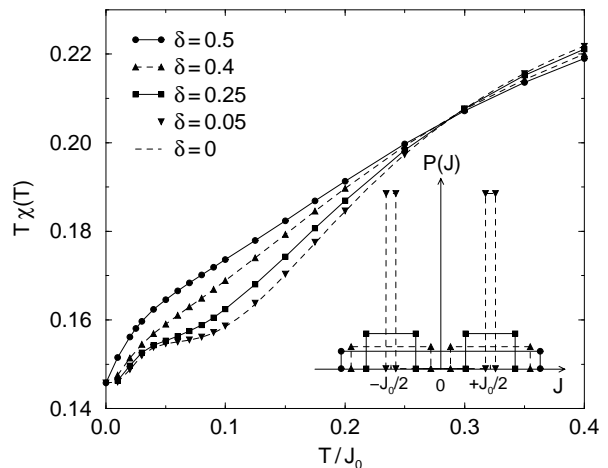


FIG. 4. Temperature dependence of the uniform Curie constant  $T\chi(T)$  for 4-site random spin chains with initial coupling distribution function Eq. (12) shown in the inset. The difference between the Curie constant for the case  $\delta = 0.05$  and  $\delta = 0$  are smaller than the symbols.

The study of the 4-site chains, giving an idea of how the universal scaling regime is reached for different  $P(J)$ , clearly shows the advantages of our choice of a broad initial distribution  $P(J)$  [Eq. (6)] for the numerical QMC study of the low-temperature scaling regime. Reducing the energy scale, the broad distributions are renormalized quite rapidly to the fixed point coupling distribution, while in the case of the peaked distributions, first new effective spins have to be formed before entering the universal low-temperature scaling regime.

Whereas the thermodynamic properties in the intermediate temperature range and the crossover temperature to the scaling regime depend strongly on the initial coupling distribution, the low-temperature regime of random FM-AFM spin-1/2 chains itself should show universal behavior. This will be analyzed in the following, based on the scaling assumption of the RSRG method, using the

statistical cluster analysis, introduced in section 4.3, as well as the QMC results for the box distribution Eq. (6).

### B. Low-temperature Curie behavior

An important result of the RSRG approach is that the uniform susceptibility approaches a Curie-like behavior in the limit  $T \rightarrow 0$ . It is possible to determine the limiting Curie constant from the initial spin size distribution and the ratio of FM to AFM bonds<sup>16,17</sup>. The low-temperature deviations from this Curie constant give important information on the scaling properties mentioned above. For the scaling analysis we calculate the product  $T\chi(T)$  with the QMC simulation over a temperature range,  $J_0/1000 \leq T \leq J_0$  as shown in Fig. 5. According to the RSRG scheme, with lowering temperature gradually the spins correlate within clusters of growing length  $l$  (see Fig. 2). Each such cluster represents an effective spin. In our case this leads to an effective diminishing of the spin degrees of freedom such that  $T\chi(T)$ , as a measure for the still uncorrelated spins at a given temperature, decreases monotonically from the large- $T$  value of  $1/4$  (the free spin-1/2 limit). The linear dependence in the intermediate temperature range reflects the initial bond distribution  $P(J)$  in Eq. (6), as discussed above for the 4-site chains.

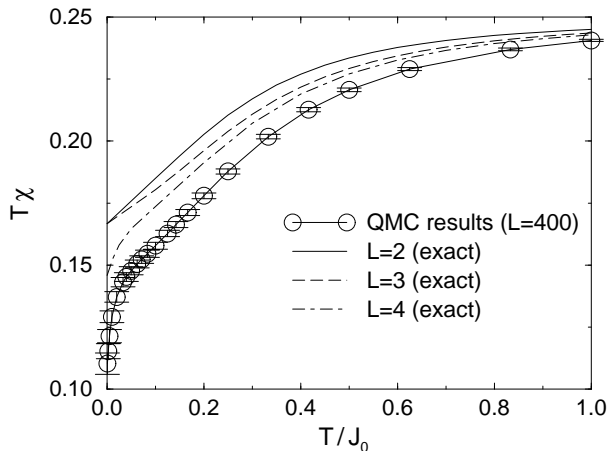


FIG. 5. QMC results for the temperature dependence of the uniform Curie constant of random FM-AFM spin-1/2 chains of length  $L = 400$  with a bond distribution according to (6). Also shown are the results for  $L = 2, 3$  and  $4$  calculated exactly by integrating over the distribution for each bond. For the small clusters open boundary conditions are used to avoid strong frustrations.

We now turn to the analysis of the low-temperature behavior of  $\chi$ . Since each cluster behaves independently we can calculate its contribution to the susceptibility and average over all cluster sizes and spin configurations. Thus

for clusters of the average length  $\bar{l}$  the Curie “constant” is given by

$$T\chi(T) = \frac{1}{\bar{l}} \sum_{l=1}^{\infty} p_{\bar{l}}(l) C_l, \quad (13)$$

where  $C_l$  is the average value of Curie constant per site for a finite, completely correlated cluster of length  $l$  which is given by the average over all possible spin quantum numbers appearing in such a cluster

$$C_l = \frac{1}{3l} \sum_{S=0}^{l/2} \rho_l(S) S(S+1). \quad (14)$$

If  $\bar{l} \gg 1$ , it is justified that we use the distribution functions  $\rho_l(S)$  and  $p_{\bar{l}}(l)$  in their continuum approximations

$$\rho_l(S) = 2\sqrt{\frac{2}{\pi l}} e^{-2S^2/l} \quad (15)$$

$$p_{\bar{l}}(l) = \frac{e^{1/(\bar{l}-1)}}{\bar{l}-1} e^{-l/(\bar{l}-1)}$$

for  $l \geq 1$ , as approximation of Eq. (10) and Eq. (11) – a comparison, done in Appendix A, of the following results with numerical results obtained using the discrete distribution shows only minor deviations even for small  $\bar{l}$ . These two distributions [Eq. (15)] are now used to calculate the low-temperature behavior of  $T\chi$

$$\begin{aligned} T\chi(T) &= \frac{1}{\bar{l}} \int_1^{\infty} dl p_{\bar{l}}(l) l C_l \\ &= \frac{1}{12} + \frac{\bar{l}^{-1/2}}{6\sqrt{2}} + O(\bar{l}^{-3/2}) \\ &= \frac{1}{12} + \frac{T^\alpha}{6\lambda\sqrt{2}} + O(T^{3\alpha}), \end{aligned} \quad (16)$$

where for the third line  $\bar{l}$  was substituted by Eq. (9).

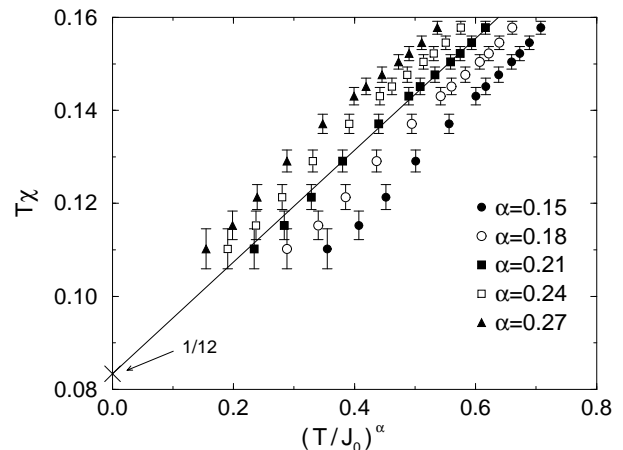


FIG. 6. Uniform Curie constant per spin as a function of  $T^\alpha$  for different  $\alpha$ . The best linear behavior [Eq. (16)] is found for  $\alpha = 0.21 \pm 0.02$ . The solid line shows a fit of form (16) for  $\alpha = 0.21$  and fixed intercept  $1/12$ . This leads to a value of  $\lambda = 1.0 \pm 0.1$ .

Fitting the two leading terms of Eq. (16) to the QMC data gives an estimate of the scaling exponent  $\alpha$  and the proportionality factor  $\lambda$ . Fig. 6 shows  $T\chi$  as a function of  $T^\alpha$  for different  $\alpha$ . Using the knowledge of the exact zero-temperature value  $1/12$  of  $T\chi$  we obtain from this plot  $\alpha = 0.21 \pm 0.02$ , in good agreement with the RSRG result  $(0.22 \pm 0.01)$ .<sup>17</sup> The proportionality factor is determined as  $\lambda = 1.0 \pm 0.1$ . These results confirm that our QMC results for chains of length  $L = 400$  are not affected by finite-size effects, because according to Eq. (9) the average length of the correlated clusters, even at the lowest simulated temperature  $J_0/1000$ , is only  $\bar{l} \approx 18$ , and therefore much smaller than  $L$ .

### C. Specific heat and entropy

The specific heat  $C$  is determined as the numerical derivative of the internal energy calculated in the QMC simulations. The errors in the specific heat increase significantly with lowering temperature. Nevertheless,  $C$  could be determined reliably down to  $T \approx J_0/150$ . The QMC results for the specific heat and the ratio  $C/T$  as a function of  $T$  are shown in Fig. 7.

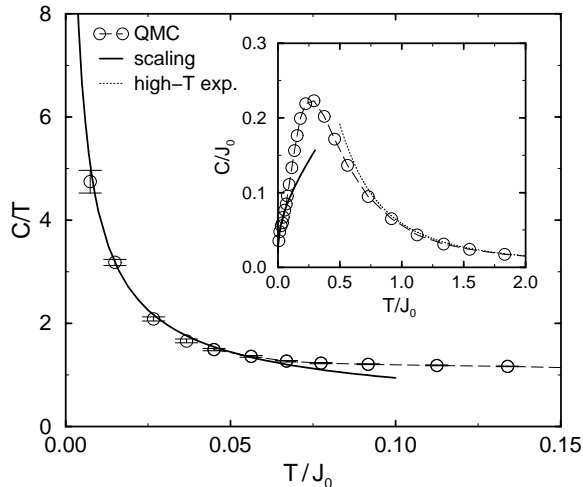


FIG. 7. Specific heat divided by temperature  $T$  as a function of  $T$ . The circles are the QMC results, while the solid line was calculated as the derivative of Eq. (18) with respect to  $T$ . The inset shows the QMC results for the specific heat as a function of temperature over a large temperature range. The error bars are smaller than the symbols.

Since  $C/T$  is the derivative of the entropy  $\sigma$  with respect to  $T$ , we may compare it to a calculation of  $\sigma$  by our statistical cluster analysis. Again we assume that for given temperature each correlated cluster behaves independently. Hence a cluster of length  $l$  contributes

$$\sigma_l = \sum_{S=0}^{l/2} \rho_l(S) \log(2S+1). \quad (17)$$

to the entropy. Here it is necessary to use the discrete expressions for the distribution functions because large deviations arise in the continuum approach using Eq. (15), instead of Eq. (10) and Eq. (11) (see Appendix A).

The entropy per site of the infinite chain is

$$\sigma(T) = \frac{1}{\bar{l}} \sum_{l=1}^{\infty} p_{\bar{l}}(l) \sigma_l, \quad (18)$$

where  $\bar{l}$  is given by Eq. (9). Using the values of  $\alpha$  and  $\lambda$  determined above, the entropy and hence  $C/T$  may be calculated from Eq. (18). The result is shown as the solid line in Fig. 7. We find good agreement with the QMC results for the low-temperature range. We emphasize that this is no fit since all free parameters have been determined via the uniform susceptibility. At higher temperatures this approach fails, because the scaling behavior Eq.(9) of  $\bar{l}$  is no longer valid.

As a further consistency check we estimate the area below the curve  $C/T$  from  $T = 0$  to  $\infty$  using  $\sigma(\infty) = \sigma(T^*) + \int_{T^*}^{\infty} dT (C/T)$ , where we set  $T^* = 0.03J_0$ . The first term is obtained using Eq. (18) and the integral from  $T^*$  to  $\infty$  is determined numerically, using the QMC results and a high temperature expansion up to third order. We find  $\sigma(\infty) = 0.68 \pm 0.01$ , in very good agreement with the expected result  $\ln 2$ . The fraction  $\sigma(T^*)$  of the entropy is large, contributing approximately 25% of the total. Therefore the fact that we find the correct value for  $\sigma(\infty)$  is a further convincing test for the correctness of Eq. (18), and of our statistical treatment of the scaling regime.

### D. Generalized staggered susceptibility

The generalized staggered susceptibility is defined here as the linear response of the spin chain to a staggered field  $H_{st}$  whose sign on site  $j$  is given by

$$\tau_j = \prod_{m=0}^{i-1} \text{sgn}(-J_m) \quad (19)$$

in analogy to the regular AFM staggering. Based on the discussion of the non-linear sigma model version of the random spin chain Nagaosa and coworkers suggested that each cluster forms a (classical) staggered spin  $s_{st}$  proportional to the cluster length  $l$ ,<sup>24</sup>

$$s_{st} = \zeta l \quad \zeta = \text{constant} \quad (20)$$

Then the staggered field  $H_{st}$  couples to  $s_{st}$  analogous to the case of a uniform field and the susceptibility should be given by the following low-temperature scaling form,

$$\chi_{\text{st}} \propto \frac{\bar{s}_{\text{st}}^2}{T\bar{l}} \propto \frac{\bar{l}}{T} \propto T^{-(1+2\alpha)}. \quad (21)$$

Using the proposed Eq. (20) and performing a similar analysis as for the uniform susceptibility, we obtain the following form

$$\chi_{\text{st}} = \frac{\zeta^2 \lambda^2}{3} T^{-(1+2\alpha)} + \frac{\zeta - 2\zeta^2}{3} T^{-1} + O(T^{-1+2\alpha}). \quad (22)$$

However, no  $\zeta$  can be found such that Eq. (22) fits our QMC data. Indeed, the low-temperature behavior of  $\chi_{\text{st}}$  is governed by a leading powerlaw  $\chi_{\text{st}} \propto T^{-\gamma}$  with  $\gamma = 1.17 \pm 0.01$  which is clearly different from the anticipated  $1 + 2\alpha$ . One may argue that the temperatures covered by the QMC simulations are not low enough and that only at lower temperature the exponent will approach the value  $1 + 2\alpha$ . The numerical data, however, show no indication for such an increase of the exponent down to temperatures as low as  $T = J_0/1000$ .

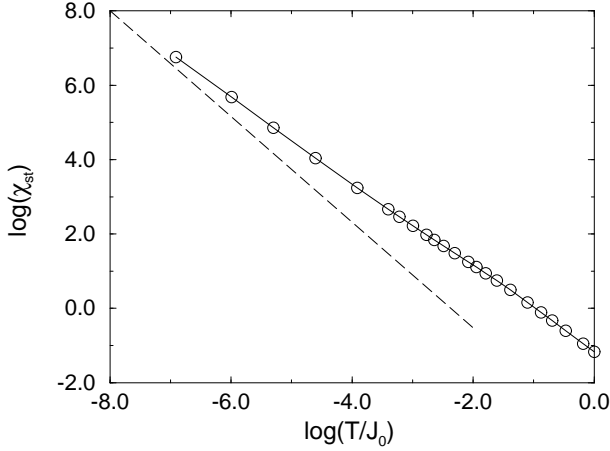


FIG. 8. Double logarithmic plot of the generalized staggered susceptibility as a function of temperature. The error bars are smaller than the symbols. The dashed line shows a divergence with  $T^{-(1+2\alpha)}$ .

This leads to the conclusion, that the assumption in Eq. (20) and Eq. (21) is not appropriate, and a revision of the ideas on the generalized staggered susceptibility is necessary.

In the following we will follow an alternative path which includes quantum effects ignored above and finally gives an overall consistent view of this problem. We consider the application of the staggered field  $H_{\text{st}}$  as a perturbation described by addition the following term to the Hamiltonian,

$$\hat{V}_{\text{st}} = -H_{\text{st}} \hat{S}_{\text{st}} = -H_{\text{st}} \sum_j \tau_j S_j^z \quad (23)$$

We now focus on the contribution of a given correlated cluster of length  $l$  to the generalized staggered susceptibility. Since the cluster is correlated it is described by its

ground state  $|\Psi_0(S, M)\rangle$  where  $(S, M)$  are the spin quantum numbers (effective spin degree of freedom). This state is, in general, not an eigenstate of  $\hat{V}_{\text{st}}$  and we find that  $\langle \Psi_0(S, M) | \hat{S}_{\text{st}} | \Psi_0(S, M) \rangle$  grows with cluster size at most as  $l^{1/2}$  (see Appendix B). As we will see below this leads to a Curie or sub-Curie law of the generalized staggered susceptibility. Therefore, we include the second order in perturbation,

$$\Delta E_M = -H_{\text{st}} \langle \Psi_0(S, M) | \hat{S}_{\text{st}} | \Psi_0(S, M) \rangle - H_{\text{st}}^2 \sum_n \frac{|\langle \Psi_0(S, M) | \hat{S}_{\text{st}} | \psi_n \rangle|^2}{\epsilon_n - \epsilon_0} \quad (24)$$

$$\equiv -H_{\text{st}} e_{M1} - H_{\text{st}}^2 e_{M2}, \quad (25)$$

where  $|\psi_n\rangle$  denotes the excited state with energy  $\epsilon_n$  and  $\epsilon_0$  is the ground state energy.

The temperature dependence of the generalized staggered susceptibility is easily calculated from the free energy of the cluster,

$$F_S = -k_B T \ln Z_S, \quad Z_S = \sum_{M=-S}^S e^{-\Delta E_M / k_B T}. \quad (26)$$

Note that other contributions to the partition function  $Z$  are of the order  $e^{-\Delta_0 / k_B T}$  and can be ignored ( $\Delta_0$  ( $\sim k_B T$ ) the excitation gap of the cluster). The generalized staggered susceptibility per spin in the cluster is then defined as

$$\chi_{\text{st}} = \frac{1}{l} \left. \frac{\partial^2 F}{\partial H_{\text{st}}^2} \right|_{H_{\text{st}}=0} = \frac{1}{(2S+1)l} \sum_{M=-S}^S \left( \frac{e_{M1}^2}{k_B T} + 2e_{M2} \right) \quad (27)$$

Now let us give upper bounds to the two terms. For  $e_{M1}$  we find

$$e_{M1} \leq g_1 l^{\rho/2} \quad (28)$$

independent of  $M$  with a constant  $g_1$  and the exponent  $\rho/2$  (see Appendix B). This upper bound is connected with the following estimate of  $e_{M2}$  which contains two elements the denominator and the numerator. The denominator has a simple lower bound  $\epsilon_n - \epsilon_0 \geq \Delta_0$ . An upper bound of the numerator is obtained if the sum over  $n$  is extended to run also over the states  $|\Psi_0(S, M)\rangle$ , leading to

$$e_{M2} \leq \frac{\langle \Psi_0(S, M) | \hat{S}_{\text{st}} \hat{S}_{\text{st}} | \Psi_0(S, M) \rangle}{\Delta_0} = \frac{1}{\Delta_0} \sum_{i,j} \tau_i \tau_j \langle \Psi_0(S, M) | S_i^z S_j^z | \Psi_0(S, M) \rangle. \quad (29)$$

This leads us to the discussion of the generalized staggered correlation function which we assume to be bounded as



$$\sum_{i,j} \tau_i \tau_j \langle \Psi_0(S, M) | S_i^z S_j^z | \Psi_0(S, M) \rangle \leq g_2 l^\rho \quad (30)$$

where  $g_2$  is a constant and  $\rho$  a scaling exponent. It is easy to see that  $\rho = 2$  for “long-range ordered” clusters and  $\rho = 1$  for short range correlation. An intermediate  $\rho$  indicates a correlation function which decays with a powerlaw,

$$\Gamma_0(r) = \sum_i \tau_i \tau_{i+r} \langle \Psi_0(S, M) | S_i^z S_{i+r}^z | \Psi_0(S, M) \rangle \propto r^{-\eta} \quad (31)$$

for large  $r$  and  $l$  what leads to  $\rho = 2 - \eta$ . Combining these estimates the generalized staggered susceptibility gets the following upper bound from the two terms,  $\chi_{\text{st}} = \chi_1 + \chi_2$ ,

$$\chi_1 = \sum_M \frac{e_{M1}^2}{(2S+1)lk_B T} \leq \text{const} \frac{l^{\rho-1}}{T} \propto T^{-(1+2\alpha(\rho-1))},$$

$$\chi_2 = \sum_M \frac{e_{M2}}{(2S+1)l} \leq \text{const} \frac{l^{\rho-1}}{\Delta_0} \propto T^{-(1+2\alpha(\rho-1))}, \quad (32)$$

where we took  $\Delta_0 \sim k_B T$  and  $l \sim \bar{l} \propto \Delta_0^{-2\alpha}$ . Since  $\eta = 0$  is a lower bound for  $\eta$  we find that the exponent of  $\chi_{\text{st}} \propto T^{-\gamma}$  lies between 1 and  $1 + 2\alpha$ . Furthermore the knowledge of  $\gamma$  from our numerical calculation allows us now to give an upper bound on the exponent  $\eta$  ( $\gamma = 1.17 \pm 0.01$  from Fig. 8),

$$\left. \begin{array}{l} \gamma \leq 1 + 2\alpha(\rho - 1) \\ \rho = 2 - \eta \end{array} \right\} \rightarrow \eta \leq 1 - \frac{\gamma - 1}{2\alpha} \approx 0.62 \pm 0.02 \quad (33)$$

This result is consistent with a recent calculation of the correlation function of large clusters using the density matrix renormalization group method by Hikihara and coworkers.<sup>25</sup> Determining the correlation function of the ground state averaged over many samples they found a powerlaw with  $\eta \approx 0.4 - 0.5$ . We will also see that our following data fit well into this interpretation. Hence we can conclude that the correlation is longer ranged than in a regular AFM spin-1/2 chain where the exponent is 1. On the other hand, the exponent of  $\chi_{\text{st}}$ , smaller than  $1 + 2\alpha$ , is inconsistent with the assumption that the ground state of the random FM-AFM chain has long range order.

### E. Correlations and generalized staggered magnetization

Finally, we calculate the correlation function

$$\Gamma(r) = \left\langle \frac{1}{L} \sum_{i=1}^L S_i^z S_{i+r}^z \left( \prod_{m=i}^{i+r-1} \text{sgn}(-J_m) \right) \right\rangle \quad (34)$$

for temperatures  $J_0/400 < T < J_0$ , using the QMC algorithm. For large  $r$  and at fixed temperature  $T$ , the correlation function  $\Gamma(r, T)$  is found to be rather well described by a pure exponential form

$$\Gamma(r, T) = R(T) e^{-r/\xi(T)}, \quad r \gg \xi(T). \quad (35)$$

$\xi(T)$  is the correlation length and the prefactor  $R(T)$  is  $r$  independent. Fitting Eq. (35) to the QMC data, leads to an estimate of  $\xi(T)$  and  $R(T)$ . The correlation length as function of temperature is shown in Fig. 9 which diverges for  $T \rightarrow 0$  with the approximate powerlaw,

$$\xi(T) \propto T^{-0.46}. \quad (36)$$

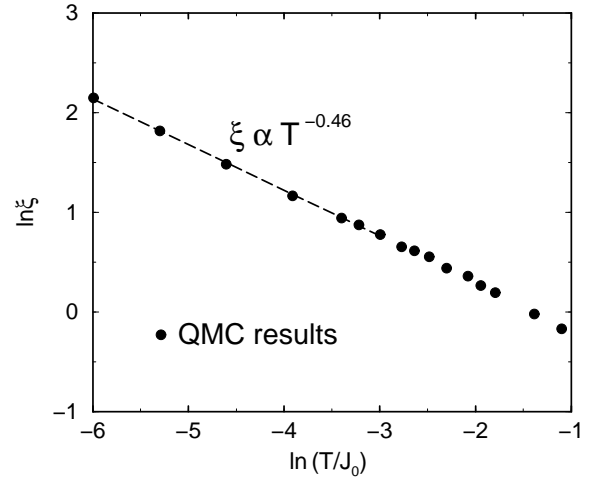


FIG. 9. Double logarithmic plot of the correlation length  $\xi$  as function of temperature  $T$ .  $\xi(T)$  diverges approximately with  $T^{-0.46}$  (dashed line) for  $T \rightarrow 0$ . The error bars are smaller or of order of the symbols.

Following the concept of our statistical cluster analysis, the correlation length  $\xi(T)$ , a measure of distance within spins are correlated in the random spin chain, should be proportional to the average cluster length  $\bar{l}$ . From this point of view we therefore expect a low temperature behavior according to

$$\xi \propto \bar{l} \propto T^{-2\alpha}. \quad (37)$$

Putting in the value  $\alpha = 0.21 \pm 0.02$ , determined before, a divergence of  $\xi(T) \propto T^{-0.42 \pm 0.04}$  is predicted, in reasonable agreement with the observed divergence, Eq. (36). After considering the length scale of the correlation function we now turn to the amplitudes.

We propose the following scaling behavior for the correlation function of random FM-AFM spin chains (for  $T \rightarrow 0$ ):

$$\Gamma(r) = \xi^\nu \tilde{\Gamma}(r/\xi), \quad \left( \frac{r}{\xi} \gg 1 \right) \quad (38)$$

where  $\tilde{\Gamma}(x)$  is a universal (temperature independent) function.

As a consequence, comparing Eq. (35) to Eq. (38), at low temperatures, the prefactor  $R(T)$  should behave as  $\xi(T)^\nu$ , leading to

$$\begin{aligned} \ln R(T) - \ln R(T_0) &= \nu \ln \xi - \nu \ln \xi_0 \\ &= -2\nu\alpha \ln T + 2\nu\alpha \ln T_0, \end{aligned} \quad (39)$$

where  $R(T_0)$  and  $\xi_0$  is the prefactor of the correlation and the correlation length, respectively, at fixed temperature  $T_0$  [c.f. Eq. (35)]. In Fig. 10 the logarithm of the prefactor  $R$  is shown as function of  $\ln T$ , at very low temperatures. The slope  $-2\alpha\nu$  is  $0.28 \pm 0.02$ , leading to a first estimate of  $\nu = -0.61 \pm 0.06$ .

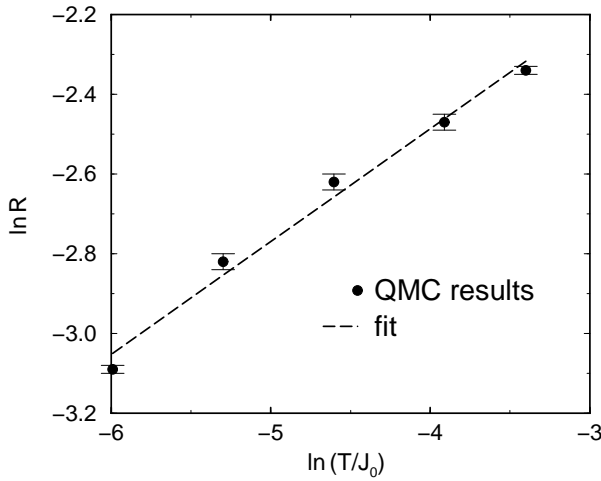


FIG. 10. Double logarithmic plot of the prefactor of the correlation function  $R$  as function of temperature  $T$  [cf. Eq. (35) and Eq. (39)]. The slope is  $-2\nu\alpha = 0.28 \pm 0.02$  (dashed line), leading to an estimate of  $\nu = -0.61 \pm 0.06$ .

Another possibility to estimate the exponent  $\nu$  is to consider the low-temperature behavior of the square of the generalized staggered magnetization defined by

$$M_{\text{st}}^2 = \left\langle \left( \frac{1}{L} \sum_{i=1}^L \tau_i S_i^z \right)^2 \right\rangle \quad (40)$$

$$= \frac{2}{L} \left( \sum_{r>0} \Gamma(r) + \frac{\Gamma(0)}{2} \right) \quad (41)$$

$$\approx \frac{2}{L} \int_0^\infty dr \Gamma(r) \quad (L \gg \xi \gg 1), \quad (42)$$

where we replaced the sum by an integral and assumed  $\xi \gg 1$  (i.e. very low  $T$ ). This allows us to neglect the term  $\Gamma(0)/2L$ .

Using the scaling form Eq. (38) for  $\Gamma(r)$  in Eq. (42) we obtain,

$$M_{\text{st}}^2 = \frac{2}{L} \xi^\nu \int_0^\infty dr \tilde{\Gamma}(r/\xi) \quad (43)$$

$$= \frac{2}{L} \xi^{\nu+1} \int_0^\infty dx \tilde{\Gamma}(x). \quad (44)$$

As the function  $\tilde{\Gamma}(x)$  is temperature independent, the square of the generalized staggered magnetization should diverge as

$$M_{\text{st}}^2 \propto \xi^{\nu+1} \propto T^{-2\alpha(\nu+1)}. \quad (45)$$

The QMC data of the square of the generalized staggered susceptibility is shown in Fig. 11. The numerical results show a divergence of  $M_{\text{st}}^2 \propto T^{-0.180 \pm 0.002}$ . From this we find for the exponent  $\nu \approx -0.61$  which is in good agreement with the previous result, deduced from the prefactor of the correlation. Note, however, that we estimate a rather large error of about 15% for  $\nu$ , as a consequence of the uncontrolled approximation performed by replacing the sum by an integral in Eq. (41) and neglecting the term  $\Gamma(0)/2L$ .

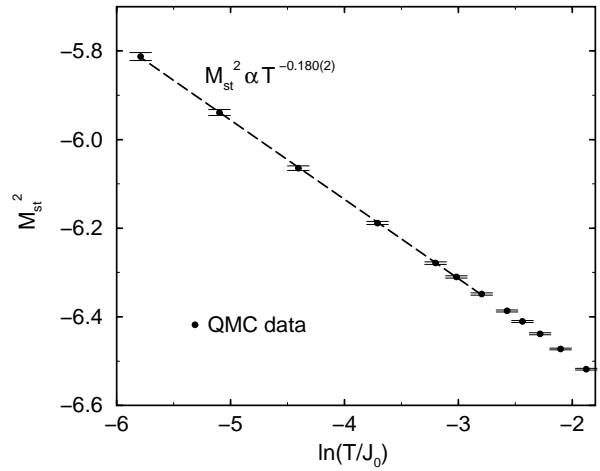


FIG. 11. Double logarithmic plot of the square of the generalized staggered magnetization  $M_{\text{st}}^2$  as function of temperature  $T$ .  $M_{\text{st}}^2$  diverges with  $T^{-0.180 \pm 0.002}$  (dashed line) for  $T \rightarrow 0$ .

Our QMC results show that the scaling behavior of the correlation function  $\Gamma(r)$  of the FM AFM random spin chains is of the form of Eq. (38). The exponent  $\nu$  is roughly estimated  $\nu = -0.61 \pm 0.06$  and is a third exponent (apart from  $\alpha$  and  $\gamma$ ) describing the low temperature scaling regime of random FM-AFM spin chains.

The exponent  $\nu$  is related to the correlation function used for the estimate of the generalized staggered susceptibility. We would like to give here a brief argument for the scaling form in Eq. (38). We consider a given distribution of clusters for fixed temperature, and average cluster length  $\bar{l}$  with the distribution function in Eq.

(15). From the assumption that the clusters are completely uncorrelated we derive the following approximation for the generalized staggered correlation function for distance  $r \gg \bar{l}$

$$\Gamma(r) \propto \int_r^\infty dl p_{\bar{l}}(l) r^{-\eta} \propto r^{-\eta} e^{-r/\bar{l}}. \quad (46)$$

Here only clusters of length larger than  $r$  can contribute and give on the average a value scaling with  $r$  as  $r^{-\eta}$  [ground state correlation within the cluster, see Eq. (31)]. Naively we might assume that  $\eta$  and  $\nu$  are identical. However, the numerical calculations show that the coherence length is shorter than the average cluster length ( $\xi \approx 2\bar{l}/3$ ) although their temperature dependence is apparently the same. The form given in Eq. (46) may be interpreted as an upper bound which does not account properly for the thermal fluctuation effects in the (most important) long clusters whose excitation gap is of the same order as the temperature.

## V. CONCLUSIONS AND SUMMARY

In the study of the random FM-AFM spin-1/2 chain, the continuous time version of the powerful quantum Monte Carlo loop algorithm allowed us to reach temperatures where clear characteristics of the universal low-energy properties of this system are observable. The characteristic temperature where the scaling behavior begins depends on the initial distribution of bond strengths. The choice of a non-singular distribution has the advantage that this temperature regime is well accessible with our simulation techniques. The key feature for analyzing the low-temperature data lies in the fact that the spins are correlated within clusters whose length grows with decreasing temperature. The scaling of the average length  $\bar{l} = \lambda^2(T/J_0)^{-2\alpha}$  and the statistics of the effective spin distribution allow a very good analysis of the numerical data. We determine both the prefactor and the exponent. The latter is assumed to be universal and agrees surprisingly well with the exponent found by the RSRG,  $\alpha = 0.21 \pm 0.02$ .<sup>16,17</sup> These two parameters ( $\alpha$  and  $\lambda$ ) are sufficient to describe the uniform susceptibility, entropy and specific heat in the whole low-temperature scaling regime.

A property not accessible by the RSRG method mentioned above is the generalized staggered susceptibility. In our simulation we show that a new exponent  $\gamma$  appears, describing the low-temperature behavior,  $\chi_{st} \propto T^{-\gamma}$  with a value  $\gamma \approx 1.17$ . A further exponent  $\nu$  arises from the scaling form of the correlation function Eq. (38). We have shown that  $\nu$  ( $\approx 0.61$ ) is connected with the ground state correlation function which probably exhibits a powerlaw decay over long distances,  $\Gamma_0(r) \propto r^{-\eta} < r^{-\nu}$ . Both exponents are assumed to be universal like  $\alpha$ , since they are derived from the properties in the low-temperature scaling regime. At present,

however, we cannot estimate the accuracy of the derived values. There is also no obvious relation between  $\gamma$ ,  $\nu$  and  $\alpha$ .

Since in the low-temperature regime the system consists of effective spin degrees of freedom which become more and more classical in their nature<sup>24</sup>, there is a clear tendency towards order in the ground state. The question is whether the remaining quantum effects (fluctuations) are sufficient to destroy long range order, here. Therefore, the important result, besides confirming the physical picture obtained by the RSRG scheme, is the fact that we do not find any indication that the ground state has long range order. The generalized staggered susceptibility as well as  $M_{st}^2$  show too increase too slowly at low temperatures. Nevertheless, the correlations must be clearly longer ranged than in the uniform AFM quantum spin-1/2 chain whose ground state staggered correlation function behaves as  $\Gamma_0(r) \propto r^{-1}$ . This finding is consistent with a recent density matrix renormalization group study and an improved version of the real space renormalization group scheme by Hikihara *et al.*<sup>25</sup> Their treatment, however, suggests that the correlation function might reach its real long-range behavior only at very long distances which we do not access in our finite temperature calculation ( $\bar{\ell} < 20$ ).

Among the (unfrustrated) random spin chains with complete spin rotation symmetry there are only two distinct classes, the ones with the random singlet phase fixed point and the others which belong to the class studied here.<sup>26</sup> For the former it was shown by Fisher that the RSRG scheme describes the fixed point behavior exactly.<sup>15</sup> This was not possible so far for the random FM-AFM spin chain. Our numerical and statistical analysis, however, demonstrates very convincingly the validity of the universal scaling assumption. Finally, we would like to emphasize that our statistical fitting procedure is very suitable and useful to analyze not only numerical, but also experimental results of this class of random spin systems.

## ACKNOWLEDGEMENTS

We would like to thank A. Furusaki, P.A. Lee, N. Nagaosa, T.M. Rice and E. Westerberg for many fruitful discussions. One of us (B.F.) is also grateful for financial support from the Swiss Nationalfonds. The calculations were performed on the Intel Paragon at the ETH Zürich.

## APPENDIX A: CONTINUOUS VS. DISCRETE DISTRIBUTIONS

There is one point to which attention has to be paid when using the statistical cluster analysis. For each considered observable it is necessary to investigate if for its calculation the exact form of the distributions [Eq. (10)

and (11)] have to be taken or if the approximate continuous forms Eq. (15) and the replacement of the sums by integrals is also reliable. It is clear that the second case is the more favorable one, since it gives simple results for the low-temperature behavior of the corresponding physical observable. Sums over the discrete distributions, on the other hand, usually can only be evaluated numerically. Therefore, the continuous forms Eq. (15) are preferred as long as they do not lead to a loss of precision. This is shown here for the example of the uniform Curie constant and the entropy.

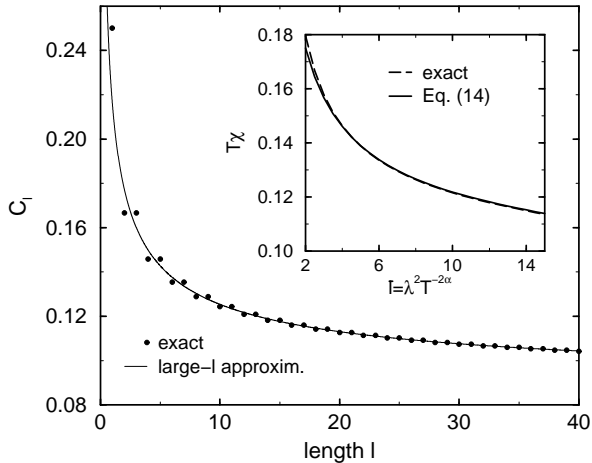


FIG. 12. Uniform Curie constant  $C_l$  per site of completely correlated clusters of length  $l$ , calculated exactly (solid points) and with large- $l$  approximation (solid line). The inset shows the Curie constant of an infinite chain as function of the average cluster length  $\bar{l}$ , calculated exactly (dashed line) and with approximate distribution  $p_{\bar{l}}$  and  $\rho_l(S)$  (solid line). For details, see text.

We first concentrate on the uniform Curie constant. The Curie constant for a completely correlated cluster as function of its length is shown in Fig. 12. It is first calculated exactly (solid points), using Eq. (14) and the discrete form Eq. (11) of  $\rho_l(S)$ . These exact results are compared to the large- $l$  approximation of  $C_l$  (solid line), which is obtained using also Eq. (14), but using the continuous approximation Eq. (15). It can be seen that this approximation is very good, also for small  $l$ . As a consequence, in Eq. (13), the approximate large- $l$  value for  $C_l$  can be used without loss of precision. The effect of replacing the exact discrete distribution  $p_{\bar{l}}(l)$  [Eq. (10)] by the continuous one [Eq. (15)] and the sum by an integral in Eq. (14), is also investigated. In the inset of Fig. 12 we show the uniform Curie constant of a random spin chain as a function of the average cluster length  $\bar{l}$ . The dashed line represents the result, obtained by using both exact (discrete) distributions [Eq. (11) and Eq. (10)] and the solid line shows the result, obtained by using both the continuous distributions Eq. (15). We find

excellent agreement for  $\bar{l} \geq 3$ , what corresponds to temperatures  $T \leq J_0/10$ . This temperature range covers the region, where the cluster distribution can be assumed to be exponential and our statistical cluster analysis results apply.

For the entropy, on the other hand, the large- $l$  approximation of  $\sigma_l$  [i.e. using the large- $l$  approximation Eq. (15) for  $\rho_l(S)$  instead of the correct distribution Eq. (11) in Eq. (18)] is very bad for small  $l$  (see Fig. 13) and it is not appropriate to use this approximation for the calculation of  $\sigma(\bar{l})$ . This can be seen in the inset of Fig. 13, where we plotted the exact value  $\sigma(\bar{l})$  (dashed line) together with the approximated value of  $\sigma(\bar{l})$ , calculated using the large- $l$  approximation for  $\sigma_l$  (dashed line). The  $\sigma(\bar{l})$  based on the continuum approximation agrees with the exact one only for  $\bar{l} \geq 15$ , which corresponds to temperatures  $T \leq J_0/500$ . In order to compare the statistical cluster analysis results with the QMC data, it is therefore necessary to calculate the entropy exactly and not to use the large- $l$  approximation.

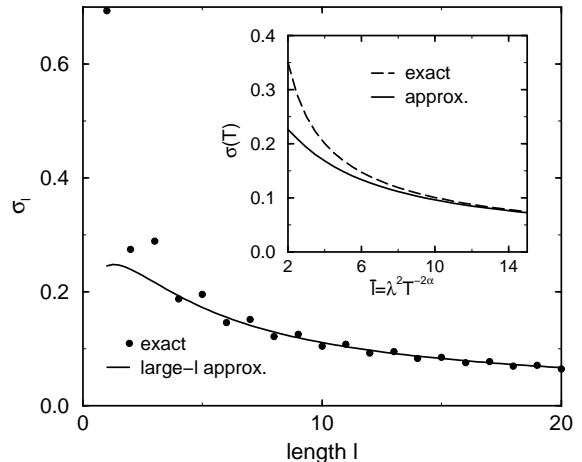


FIG. 13. Entropy contribution  $\sigma_l$  of completely correlated clusters of length  $l$ , calculated exactly (solid points) and with large- $l$  approximation (solid line). The inset shows the entropy per site of an infinite chain as function of the average cluster length  $\bar{l}$ , calculated exactly (dashed line) and with approximate distribution  $p_{\bar{l}}$  and  $\rho_l(S)$  (solid line). For details, see text.

## APPENDIX B: BOUNDS FOR THE STAGGERED MOMENTS

The aim of this section is to establish the upper bounds for  $e_{M1}$  and  $e_{M2}$  in Eq. (28) and (30), respectively, for a given cluster with the ground state  $|\Psi_0(S, M)\rangle$  of degeneracy  $2S + 1$ . The generalized staggered correlation function  $\Gamma(r)$  given in Eq. (31) is assumed to scale with the powerlaw  $r^{-\eta}$ . Therefore we find

$$\begin{aligned}
& \langle \Psi_0(S, M) | \hat{S}_{st} \hat{S}_{st} | \Psi_0(S, M) \rangle \\
&= \sum_{i,j} \tau_i \tau_j \langle \Psi_0(S, M) | S_i^z S_j^z | \Psi_0(S, M) \rangle \quad (47) \\
&= \int_0^l dr \int_0^l dr' \Gamma_{0M}(|r-r'|) \propto l^{2-\eta} = l^\rho,
\end{aligned}$$

which defines the exponent  $\rho$ . The proportionality factor  $g_2$  in Eq. (30) was chosen large enough such that  $g_2 l^\rho$  acts as an upper bound for all spin quantum numbers  $M$  for given  $S$  and  $l$ .

Now we turn to  $e_{M1}$  for which we obtain an upper bound using Eq. (47).

$$\begin{aligned}
e_{M1}^2 &= |\langle \Psi_0(S, M) | \hat{S}_{st} | \Psi_0(S, M) \rangle|^2 \\
&\leq \sum_n \langle \Psi_0(S, M) | \hat{S}_{st} | \Psi_n \rangle \langle \Psi_n | \hat{S}_{st} | \Psi_0(S, M) \rangle \quad (48) \\
&= \langle \Psi_0(S, M) | \hat{S}_{st} \hat{S}_{st} | \Psi_0(S, M) \rangle \leq g_2 l^\rho
\end{aligned}$$

where the sum runs over the complete set of basis states  $|\Psi_n\rangle$  including, of course,  $|\Psi_0(S, M)\rangle$ . Taking the square root we obtain the upper bound for  $e_{M1}$  with  $g_1 \geq \sqrt{g_2}$ .

- <sup>14</sup> J.E. Hirsch, Phys. Rev. B **22** (1980) 5355.  
<sup>15</sup> D.S. Fisher, Phys. Rev. B **50** (1994) 3799.  
<sup>16</sup> E. Westerberg, A. Furusaki, M. Sigrist and P.A. Lee, Phys. Rev. Lett. **75** (1995) 4302.  
<sup>17</sup> E. Westerberg, A. Furusaki, M. Sigrist and P.A. Lee, Phys. Rev. B **55**, 12578 (1997).  
<sup>18</sup> K.Hida, J. Phys. Soc. Jpn. **66**, 330 (1997).  
<sup>19</sup> B. Frischmuth, and M. Sigrist, Phys. Rev. Lett. **79**, 147 (1997).  
<sup>20</sup> H.G. Evertz, G. Lana, and M. Marcu, Phys. Rev. Lett. **70**, 875 (1993)  
<sup>21</sup> B.B. Beard and U.-J. Wiese, Phys. Rev. Lett. **77** (1996) 5130.  
<sup>22</sup> B. Ammon, and M. Sigrist, in preparation.  
<sup>23</sup> W. Marshall, Proc. R. Soc. London Ser. **A 232**, 48 (1955); E. Lieb and D.C. Mattis, J. Math. Phys. **3**, 749 (1962).  
<sup>24</sup> N. Nagaosa, A. Furusaki, M. Sigrist, and H. Fukuyama, J. Phys. Soc. Jpn. **65** (1996) 3724.  
<sup>25</sup> T. Hikiyama, A. Furusaki and M. Sigrist, unpublished.  
<sup>26</sup> Random spin chains whose bond distribution functions are very singular in the limit  $J \rightarrow 0$  are excluded from this classification. For these systems, usually no universal scaling regime can be reached and the low-temperature behavior is governed by the  $J \rightarrow 0$ -limit of the initial bond distribution.

- 
- <sup>1</sup> J.P. Renard *et al.*, J. Appl. Phys. **63**, 3538 (1988); M. Date and K. Kindo, Phys. Rev. Lett. **65**, 1659 (1990).  
<sup>2</sup> J.S. Miller (editor), *Extended Linear Chain Compounds*, Vol. 3, Plenum Press, New York, 1983.  
<sup>3</sup> A.P. Wilkinson, and A.K. Cheetham, Acta Cryst. C **45**, 1672 (1989); A.P. Wilkinson, A.K. Cheetham, W. Kunnman, and A. Kvik, Eur. J. Solid State Inorg. Chem. **28**, 453 (1991).  
<sup>4</sup> For a review, see E. Dagotto and T.M. Rice, Science **271** (1996) 618.  
<sup>5</sup> C.A. Doty and D.S. Fisher, Phys. Rev. B **45**, 2167 (1992); see also K.J. Runge and G.T. Zimanyi, *ibid.*, **49**, 15212 (1994) and references therein.  
<sup>6</sup> T.N. Nguyen, P.A. Lee, and H.-C. zur Loye, Science **271**, 489 (1996).  
<sup>7</sup> A. Furusaki, M. Sigrist, P.A. Lee, K. Tanaka, and N. Nagaosa, Phys. Rev. Lett. **73**, 2622 (1994); A. Furusaki, M. Sigrist, E. Westerberg, P.A. Lee, K.B. Tanaka and N. Nagaosa, Phys. Rev. B, **52**, 15930 (1995).  
<sup>8</sup> H. Fukuyama, T. Tanimoto and M. Saito, J. Phys. Soc. Jpn. **65** (1996) 1183; H. Fukuyama, N. Nagaosa, M. Saito and T. Tanimoto, J. Phys. Soc. Jpn. **65** (1996) 2377.  
<sup>9</sup> M. Sigrist and A. Furusaki, J. Phys. Soc. Jpn. **65**, 2385 (1996).  
<sup>10</sup> K. Yang and R.N. Bhatt, unpublished.  
<sup>11</sup> C. Dasgupta and S.-k. Ma, Phys. Rev. B **22** (1980) 1305.  
<sup>12</sup> S.-k. Ma, C. Dasgupta, and C.K. Hu, Phys. Rev. Lett. **43** (1979) 1434.  
<sup>13</sup> J.E. Hirsch and J.V. Jose, Phys. Rev. B **22** (1980) 5339.